

# Development of 3-Dimensional Position/Attitude Determination Radio-navigation System with FLAOA and TOA Measurements

Jong-Hwa Jeon<sup>1</sup>, Jeong-Min Lim<sup>2</sup>, Sang-Hoon Yoo<sup>3</sup>, Tae-Kyung Sung<sup>1†</sup>

<sup>1</sup>Department of Electronics, Radio Sciences and Information Communications Engineering, Chungnam National University, Daejeon 34140, Korea

<sup>2</sup>MTG Co. Ltd, Daejeon 34068, Korea

<sup>3</sup>WiFive Co. Ltd, Daejeon 34183, Korea

## ABSTRACT

Existing radio positioning systems have a drawback that the attitude of user's tag is difficult to be determined. Although forward link angle of arrival (FLAOA) technology that uses measurements of array antenna arranged in a tag among the angle of arrival (AOA) technologies can estimate attitude and positioning of tags, it cannot extend the estimated results into three-dimensional (3D) results due to complex non-linear model displayed because of the effects of 3D positioning and attitude in tags. This paper proposed a radio navigation technique that determines 3D attitude and positioning via FLAOA / time of arrival (TOA) integration. According to the order of determining attitude and positioning, two integration techniques were proposed. To analyze the performance of the proposed technique, MATLAB-based simulations were used to verify the performance. The simulation results showed that the first proposed method, TOA-FLAOA integrated technique, showed about 0.15 m of positioning error, and 2–3° of attitude error performances regardless of the positioning space size whereas the second method, differenced FLAOA-TOA integrated technique, revealed a problem that a positioning error became larger as the size of the positioning space became larger.

**Keywords:** FLAOA, TOA, AOA, attitude, positioning

## 1. INTRODUCTION

In recent years, a variety of application systems based on radio navigation that ensures high-level accuracy and availability in the outdoor for users around the world have been widely used due to the constant deployment of various global navigation satellite systems (GNSS). However, GNSS-based positioning systems have a drawback that they cannot be used in the indoor and various radio navigation-based positioning technologies such as Wi-Fi, bluetooth low energy (BLE), and Impulse radio-ultra wide band (IR-UWB) have been developed for indoor positioning (Hu 2013, Zhu et al. 2014). The positioning technologies based on Wi-Fi or BLE

have several to tens of meters of positioning error in the indoor due to the effect of poor indoor radio environment. Thus, IR-UWB based radio positioning technology has been widely used in the high precision positioning application area (Sahinoglu 2008, Viot 2014).

The high precision positioning and attitude information of vehicle is necessary to control unmanned vehicles precisely in a large sized indoor environment such as smart factory, logistic warehouse, and public facilities. The previous study employed fusion of sensors such as Inertial Navigation System and Compass to determine indoor attitude of tag (Hu 2013), but the sensor-based positioning had a drawback of accumulation of errors over time and it is affected by the indoor environment significantly (Zhu et al. 2014). In addition, existing radio navigation-based indoor positioning systems can be employed in a wide positioning space and determine a position of tag via inexpensive equipment but they have a problem of providing only tag positioning without

---

Received Feb 14, 2018 Revised Mar 25, 2018 Accepted Mar 26, 2018

†Corresponding Author

E-mail: tksaint@cnu.ac.kr

Tel: +82-42-821-5660 Fax: +82-42-824-6807

attitude information.

The radio navigation of angle of arrival (AOA) mode using angle measurements can be divided into two: reverse link AOA (RLAOA) and forward link AOA (FLAOA) according to the installation location of array antennas. In RLAOA, array antennas are arranged in the access point (AP) installed in the fixed location, and positioning of the tag can be calculated through distance and angle measurements acquired from the array antennas. However, attitude of the moving signal source cannot be determined in the case of RLAOA (Kim et al. 2007). In contrast, array antennas are installed in the moving tag in FLAOA and angle measurements acquired here are determined according to the position and attitude of the tag. Therefore, it is possible to estimate the position and attitude of the tag by using the FLAOA measurement. (Kim et al. 2007, Song et al. 2009). However, it is difficult to obtain the analytical solution in the case of FLAOA measurements due to the complex nonlinearity of the angle measurements. Thus, previous studies on FLAOA have been focused on two-dimensional (2D) positioning and attitude estimation techniques (Song et al. 2009).

This paper proposed an FLAOA/TOA integrated technique that determined 3D attitude and positioning by integrating FLAOA and TOA measurements for 3D attitude and positioning determination of tags. Two analytical solution methods were induced to determine 3D positioning and attitude thereby showing the possibility of determining 3D attitude and positioning of the tag via radio navigation. Section 2 introduces AOA measurements and existing 2D FLAOA-based positioning techniques. Section 3 explains the proposed technique in this paper that determines 3D attitude and positioning by integrating FLAOA and TOA. Section 4 compares and analyzes the performances of the proposed two integration techniques, and finally, Section 5 presents the conclusions.

## 2. 2D FLAOA-BASED POSITIONING

### 2.1 AOA Measurement Model

In order to obtain AOA measurement, which is an angle information in the direction where the signal source is located, array antennas with more than 2 antenna elements have to be used, and user's direction that generates signals can be estimated using a difference in signal arrival times obtained from each of the antenna elements. Assuming that the AP and signal source are far enough away from each other that the AP views the signals from the signal generation source as parallel waves, the simplest structure that can

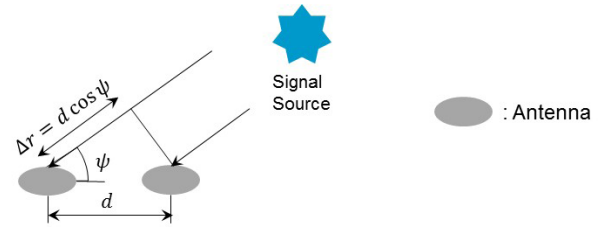


Fig. 1. Two-dimensional AOA measurement model.

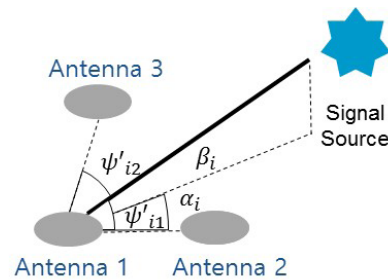


Fig. 2. Structure of array antennas for three-dimensional estimation.

obtain AOA measurements of signal source from the AP is shown in Fig. 1 in which two antennas are used.

As shown in Fig. 1, an angle ( $\psi$ ) where the user is located within the 2D half-plane can be estimated in the case of AOA of the simplest structure using only two antennas. Here,  $d$  refers to a gap between two antennas, and  $\Delta r$  refers to a difference in distance between received signals arrived at two antennas.

In the case of 3D AOA measurements, three or more antenna elements are needed, and they should not be located in the same line. The structure of array antennas in which three antenna elements are mutually orthogonal is shown in Fig. 2. The signal source may not exist in the plane made by two baseline vectors between antenna elements in 3D antenna. Azimuth  $\alpha_i$  and elevation  $\beta_i$ , which is a 3D solid angle with regard to the signal source, can be calculated via Eq. (1) using an incident angle  $\psi'_{i1}$  measured from Antennas 1 and 2 and an incident angle  $\psi'_{i2}$  measured from Antennas 1 and 3 (Mardiana & Kawasaki 2000).

$$\begin{aligned} \cos \psi'_{i1} &= \cos \beta_i \cos \alpha_i \\ \cos \psi'_{i2} &= \cos \beta_i \sin \alpha_i \end{aligned} \tag{1}$$

The AOA (mode) can be divided into RLAOA and FLAOA (modes) depending on the main actor that measures the arrival angle of the received signal. In RLAOA, array antennas are installed in AP and a location of the tag can be acquired using distance and angle measurements of the array antenna. The 2D RLAOA measures an angle of arrival ( $\psi_i$ ) at the  $i$ -th AP where the array antenna is installed when a user receives a signal as shown in Fig. 3, and from this  $\psi_i$  and the  $i$ -th AP location  $(x_p, y_p)$ , location  $(x_u, y_u)$  of the user can be estimated

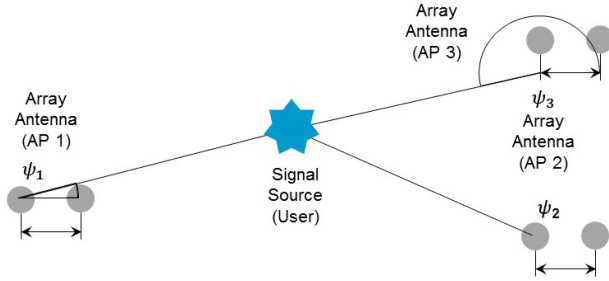


Fig. 3. Two-dimensional RLAA based localization.

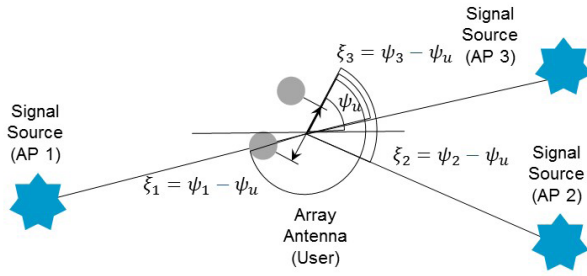


Fig. 4. Two-dimensional FLAOA based localization.

(Song et al. 2009).

The 2D RLAA measurement model is presented in Eq. (2). In the case of RLAA, the attitude of the signal source is not included in the angle measurement so that the attitude of the user cannot be calculated (Kim et al. 2007).

$$\psi_i = \tan^{-1} \left( \frac{y_u - y_i}{x_u - x_i} \right) \quad (2)$$

In FLAOA, an array antenna is installed in the moving tag, and angle measurements ( $\xi_i$ ) acquired here includes the attitude measurement ( $\psi_u$ ) of the tag as shown in Fig. 4. Thus, the position and attitude of the tag can be estimated using FLAOA measurements.

The 2D FLAOA measurement model is presented in Eq. (3) (Kim et al. 2007, Lim 2017).

$$\tan(\xi_i) = \tan(\psi_i - \psi_u) = \frac{(y_u - y_i) - (x_u - x_i) \tan \psi_u}{(x_u - x_i) + (y_u - y_i) \tan \psi_u} \quad (3)$$

## 2.2 Two-dimensional Attitude and Positioning Measurement Technique Based on FLAOA Measurements

The previous studies on 2D FLAOA reported that 2D attitude ( $\psi_u$ ) and positioning ( $x_u, y_u$ ) of the tag can be estimated analytically through the measurement transformation using the relationship equation between positioning and attitude of the tag and FLAOA measurements (Kim et al. 2007, Song et al. 2009). Eq. (3), which is a 2D FLAOA measurement of the  $i$ -th AP is summarized as Eq. (4).

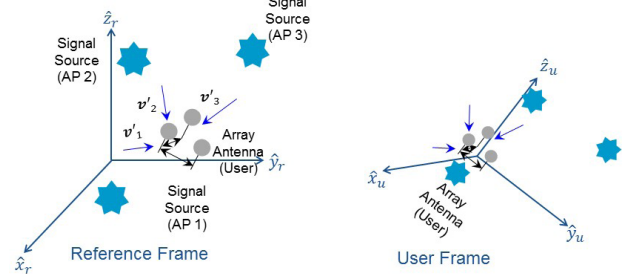


Fig. 5. Three-dimensional FLAOA based localization.

$$(x_u - x_i) \tan \xi_i + (y_u - y_i) \tan \psi_u \tan \xi_i = (y_u - y_i) - (x_u - x_i) \tan \psi_u \quad (4)$$

By defining  $r = \tan \psi_u$ ,  $p = x_u + y_u r$ , and  $q = x_u r - y_u$  and using the measurements from  $N$  APs, it is expressed as a matrix as presented in Eq. (5).

$$\begin{bmatrix} -(x_1 + y_1 \tan \xi_1) & \tan \xi_1 & 1 \\ -(x_2 + y_2 \tan \xi_2) & \tan \xi_2 & 1 \\ \vdots & \vdots & \vdots \\ -(x_N + y_N \tan \xi_N) & \tan \xi_N & 1 \end{bmatrix} \begin{bmatrix} r \\ p \\ q \end{bmatrix} = A \underline{z} = \begin{bmatrix} x_1 \tan \xi_1 - y_1 \\ x_2 \tan \xi_2 - y_2 \\ \vdots \\ x_N \tan \xi_N - y_N \end{bmatrix} = \underline{b} \quad (5)$$

By applying the least square to Eq. (5),  $r$ ,  $p$ , and  $q$ , which are unknown parameters, can be estimated as presented in Eq. (6).

$$\underline{z} = \begin{bmatrix} r \\ p \\ q \end{bmatrix} = (A^T A)^{-1} A^T \underline{b} \quad (6)$$

From the estimated  $r$ ,  $p$ , and  $q$ , positioning ( $x_u, y_u$ ) and attitude ( $\psi_u$ ) of the tag are calculated via Eq. (7).

$$x_u = \frac{p + rq}{1 + r^2}, \quad y_u = \frac{rp - q}{1 + r^2}, \quad \psi_u = \tan^{-1} r \quad (7)$$

## 3. TECHNIQUE TO DETERMINE 3D ATTITUDE AND POSITIONING BASED ON FLAOA/TOA

### 3.1 Three-dimensional FLAOA/TOA Measurement Model

Since 3D FLAOA measurement is affected not only by tag location but also by 3D attitude between reference and tag coordinates as shown in Fig. 5, it is determined by six variables. That is, it is expressed as a complex non-linear measurement model where roll angle ( $\phi_u$ ), pitch angle ( $\theta_u$ ), and yaw angle ( $\psi_u$ ), which are 3D attitude measurements of the tag that needs estimation, are multiplied one another, and the 3D FLAOA/TOA measurements are presented in Eq. (8) (Lim 2017).

$$\begin{bmatrix} \frac{(x_i - x_u)}{\rho_i} \\ \frac{(y_i - y_u)}{\rho_i} \\ \frac{(z_i - z_u)}{\rho_i} \end{bmatrix} = T(\psi_u)T(\theta_u)T(\phi_u) \begin{bmatrix} \cos \beta_i \cos \alpha_i \\ \cos \beta_i \sin \alpha_i \\ \sin \beta_i \end{bmatrix} \quad (8)$$

Here,  $[\cos \beta_i \cos \alpha_i \cos \beta_i \sin \alpha_i \sin \beta_i]^T$  refers to 3D FLAOA measurement measured at the tag, and  $(\phi_u, \theta_u, \psi_u)$  refers to roll angle, pitch angle, and yaw angle that represent a rotation between the reference and tag coordinates. In addition,  $(x_i, y_i, z_i)$  refers to a position of the  $i$ -th AP in the reference coordinate,  $(x_u, y_u, z_u)$  refers to a position of the tag in the reference coordinate,  $\rho_i = \sqrt{(x_u - x_i)^2 + (y_u - y_i)^2 + (z_u - z_i)^2}$  and  $T(\psi_u)$ ,  $T(\theta_u)$ ,  $T(\phi_u)$  is calculated via Eq. (9) (Van Graas & Braasch 1991, Titterton & Weston 2004).

$$\begin{aligned} T(\phi_u) &= \begin{bmatrix} 1 & 0 & 0 \\ 0 & \cos \phi_u & -\sin \phi_u \\ 0 & \sin \phi_u & \cos \phi_u \end{bmatrix}, \\ T(\theta_u) &= \begin{bmatrix} \cos \theta_u & 0 & \sin \theta_u \\ 0 & 1 & 0 \\ -\sin \theta_u & 0 & \cos \theta_u \end{bmatrix}, \\ T(\psi_u) &= \begin{bmatrix} \cos \psi_u & -\sin \psi_u & 0 \\ \sin \psi_u & \cos \psi_u & 0 \\ 0 & 0 & 1 \end{bmatrix} \end{aligned} \quad (9)$$

The 3D FLAOA problem is to estimate unknown numbers  $(x_u, y_u, z_u, \phi_u, \theta_u, \psi_u)$  from the measurements  $(\alpha_i, \beta_i)$  from multiple APs. Since not only the position  $(x_u, y_u, z_u)$  of the tag from the 3D FLAOA measurement but also attitude  $(\phi_u, \theta_u, \psi_u)$  should be estimated, and the position and attitude are coupled complexly, it is difficult to calculate an analytical solution using FLAOA measurement only. To solve this problem, this paper proposes a technique to determine 3D position and attitude via two methods by integrating FLAOA measurement with TOA measurement.

### 3.2 Position and Attitude Determination Technique Based on TOA and FLAOA Measurements

The first technique proposed in this paper is a TOA-FLAOA integrated technique, in which the position of the tag is calculated first using TOA measurements, and then the attitude of the tag is calculated using the estimated tag position and FLAOA measurement. In order to calculate the position of the tag first based on TOA measurements, TOA measurement between the tag and the  $i$ -th AP is presented in Eq. (10).

$$\rho_i = \sqrt{(x_u - x_i)^2 + (y_u - y_i)^2 + (z_u - z_i)^2} \quad (10)$$

The position  $(x_u, y_u, z_u)$  of the tag can be estimated by applying least squares etc. to TOA measurement from N APs (Bensky 2008).

To calculate the attitude of the tag using the position of the tag estimated from TOA measurement, Eq. (8) is rewritten to become Eq. (11).

$$\begin{bmatrix} (x_i - x_u) \\ (y_i - y_u) \\ (z_i - z_u) \end{bmatrix} = T \begin{bmatrix} \rho_i \cos \beta_i \cos \alpha_i \\ \rho_i \cos \beta_i \sin \alpha_i \\ \rho_i \sin \beta_i \end{bmatrix} \quad (11)$$

Here, it satisfies

$$T = T(\psi_u)T(\theta_u)T(\phi_u) = \begin{bmatrix} \cos \psi_u \cos \theta_u & -\sin \psi_u \cos \theta_u + \cos \psi_u \sin \theta_u \sin \phi_u & \sin \psi_u \sin \theta_u \sin \phi_u & \sin \psi_u \sin \phi_u + \cos \psi_u \sin \theta_u \cos \phi_u \\ \sin \psi_u \cos \theta_u & \cos \psi_u \cos \theta_u + \sin \psi_u \sin \theta_u \sin \phi_u & -\cos \psi_u \sin \theta_u \sin \phi_u + \sin \psi_u \sin \theta_u \cos \phi_u \\ -\sin \theta_u & \cos \theta_u \sin \phi_u & \cos \theta_u \cos \phi_u \end{bmatrix}$$

(Van Graas & Braasch 1991). Assuming that the measurements are acquired from N APs, Eq. (11) is expressed as presented in Eq. (12) as a determinant.

$$\begin{bmatrix} (x_1 - x_u) & (x_2 - x_u) & \dots & (x_N - x_u) \\ (y_1 - y_u) & (y_2 - y_u) & \dots & (y_N - y_u) \\ (z_1 - z_u) & (z_2 - z_u) & \dots & (z_N - z_u) \end{bmatrix} = T \begin{bmatrix} \rho_1 \cos \beta_1 \cos \alpha_1 & \rho_2 \cos \beta_2 \cos \alpha_2 & \dots & \rho_N \cos \beta_N \cos \alpha_N \\ \rho_1 \cos \beta_1 \sin \alpha_1 & \rho_2 \cos \beta_2 \sin \alpha_2 & \dots & \rho_N \cos \beta_N \sin \alpha_N \\ \rho_1 \sin \beta_1 & \rho_2 \sin \beta_2 & \dots & \rho_N \sin \beta_N \end{bmatrix} \quad (12)$$

The rotation matrix  $T$ , which contains unknown numbers in Eq. (12) can be calculated using Eq. (13) (Van Graas & Braasch 1991, Titterton & Weston 2004).

$$T = R_{ned} R_{body}^T (R_{body} R_{body}^T)^{-1} \quad (13)$$

Here, it satisfies

$$\begin{aligned} R_{body} &= \begin{bmatrix} (x_1 - x_u) & (x_2 - x_u) & \dots & (x_N - x_u) \\ (y_1 - y_u) & (y_2 - y_u) & \dots & (y_N - y_u) \\ (z_1 - z_u) & (z_2 - z_u) & \dots & (z_N - z_u) \end{bmatrix}, \\ R_{ned} &= \begin{bmatrix} \rho_1 \cos \beta_1 \cos \alpha_1 & \rho_2 \cos \beta_2 \cos \alpha_2 & \dots & \rho_N \cos \beta_N \cos \alpha_N \\ \rho_1 \cos \beta_1 \sin \alpha_1 & \rho_2 \cos \beta_2 \sin \alpha_2 & \dots & \rho_N \cos \beta_N \sin \alpha_N \\ \rho_1 \sin \beta_1 & \rho_2 \sin \beta_2 & \dots & \rho_N \sin \beta_N \end{bmatrix} \end{aligned}$$

From  $T$  calculated via Eq. (13), the attitude  $(\phi_u, \theta_u, \psi_u)$  of the tag can be calculated as presented in Eq. (14) (Van Graas & Braasch 1991).

$$\theta_u = \sin^{-1}(-T_{31}), \phi_u = \sin^{-1}\left(\frac{T_{32}}{\cos \theta_u}\right), \psi_u = \sin^{-1}\left(\frac{T_{21}}{\cos \theta_u}\right) \quad (14)$$

Here,  $T_{ij}$  refers to the  $i$ -th row and  $j$ -th column element of the rotation matrix  $T$ .

### 3.3 Differential Attitude and Positioning Determination Technique Based on FLAOA and TOA Measurements

The second technique proposed in this paper is a differenced FLAOA-TOA integrated technique, in which the attitude of the tag is calculated first using differenced FLAOA measurements, and then the position of the tag is calculated. To estimate the attitude of the tag first, FLAOA/TOA measurement of the  $i$ -th AP is differentiated based on FLAOA/TOA measurement of the first AP to have Eq. (15).

$$\begin{aligned} \begin{bmatrix} (x_i - x_1) \\ (y_i - y_1) \\ (z_i - z_1) \end{bmatrix} &= \begin{bmatrix} (x_i - x_u) - (x_1 - x_u) \\ (y_i - y_u) - (y_1 - y_u) \\ (z_i - z_u) - (z_1 - z_u) \end{bmatrix} \\ &= T \left( \begin{bmatrix} \cos \beta_i \cos \alpha_i \\ \cos \beta_i \sin \alpha_i \\ \sin \beta_i \end{bmatrix} - \rho_1 \begin{bmatrix} \cos \beta_1 \cos \alpha_1 \\ \cos \beta_1 \sin \alpha_1 \\ \sin \beta_1 \end{bmatrix} \right) \end{aligned} \quad (15)$$

Here,  $\rho_i$  employs TOA measurement. Assuming that the measurements are acquired from N APs, Eq. (15) is used to have Eq. (16) which is a determinant.

$$\begin{aligned} R_{\text{body}}^D &= \begin{bmatrix} (x_2 - x_1) & (x_3 - x_1) & \dots & (x_n - x_1) \\ (y_2 - y_1) & (y_3 - y_1) & \dots & (y_n - y_1) \\ (z_2 - z_1) & (z_3 - z_1) & \dots & (z_n - z_1) \end{bmatrix} \\ &= T \left( \begin{bmatrix} (\rho_2 \cos \beta_2 \cos \alpha_2 - \rho_1 \cos \beta_1 \cos \alpha_1) & (\rho_3 \cos \beta_3 \cos \alpha_3 - \rho_1 \cos \beta_1 \cos \alpha_1) & \dots & (\rho_n \cos \beta_n \cos \alpha_n - \rho_1 \cos \beta_1 \cos \alpha_1) \\ (\rho_2 \cos \beta_2 \sin \alpha_2 - \rho_1 \cos \beta_1 \sin \alpha_1) & (\rho_3 \cos \beta_3 \sin \alpha_3 - \rho_1 \cos \beta_1 \sin \alpha_1) & \dots & (\rho_n \cos \beta_n \sin \alpha_n - \rho_1 \cos \beta_1 \sin \alpha_1) \\ (\rho_2 \sin \beta_2 - \rho_1 \sin \beta_1) & (\rho_3 \sin \beta_3 - \rho_1 \sin \beta_1) & \dots & (\rho_n \sin \beta_n - \rho_1 \sin \beta_1) \end{bmatrix} \right) \end{aligned} \quad (16)$$

Here,  $R_{\text{body}}^D$  and  $R_{\text{ned}}^D$  refer to the differentiated measurement and state in the body and reference coordinates, respectively. The unknown parameter is a rotation matrix  $T$  determined through the tag attitude, and  $T$  can be calculated using the same method presented in Eq. (13). After calculating  $T$ , the tag attitude  $(\phi_w, \theta_w, \psi_w)$  is calculated using the same method presented in Eq. (14). Using  $T$  calculated from Eq. (16), pre-determined position of  $i$ -th AP  $(x_p, y_p, z_p)$ , and FLAOA measurement, the position  $(x_w, y_w, z_w)$  of the tag can be calculated from Eq. (11).

The differenced FLAOA-TOA integrated technique requires the pseudo inverse operation only for attitude estimation, which is in contrast with TOA-FLAOA integrated technique. Thus, it has an advantage of fewer computations than that of TOA-FLAOA integrated technique.

## 4. SIMULATION RESULT

This section compared the performances of proposed two FLAOA/TOA integrated positioning systems through simulations. The position was calculated first through MATLAB based simulations, and the attitude was then

Table 1. Placement of APs in each experiment.

	AP	x [m]	y [m]	z [m]
Experiment 1	AP1	-2.5	-2.5	1
	AP2	-2.5	2.5	1
	AP3	2.5	-2.5	1
	AP4	2.5	2.5	1
Experiment 2	AP1	-2.5	-2.5	-1
	AP2	-2.5	-2.5	1
	AP3	-2.5	2.5	-1
	AP4	-2.5	2.5	1
	AP5	2.5	-2.5	-1
	AP6	2.5	-2.5	1
	AP7	2.5	2.5	-1
	AP8	2.5	2.5	1
Experiment 3	AP1	-5	-2.5	1
	AP2	-5	2.5	1
	AP3	5	-2.5	1
	AP4	5	2.5	1

calculated using TOA-FLAOA integrated technique for attitude calculation. Then, the positioning errors of the differential FLAOA-TOA integrated technique that calculated positioning were compared. To make the simulation have a similar significance with the actual IR-UWB positioning test, the TOA measurement deviation was set to 0.1 m (Viot 2014), and FLAOA angle measurement deviation was set to 1.5° (Swedberg 2016). For the error model, the Gaussian error model, which has been widely used in measurement error models, was applied. Since IR-UWB positioning test was assumed, Non Line of Sight (NLOS) environment and multi-path errors were ignored (Sahinoglu 2008). The test was divided into three cases according to the number of APs and arrays. The error according to the expansion of the positioning space was compared in each test case. The environment of Experiment 1 was a square type AP arrangement as a basic positioning space. Experiment 2 was the same environment but the number of APs was increased. Experiment 3 employs a rectangular type AP array to analyze the positioning performance according to dilution of precision (DOP). The coordinate of the AP in each experiment is presented in Table 1, and the layout of the APs is shown in Fig. 6. For the positioning algorithm, the Gauss-Newton (GN) technique, which is one of the most widely used methods, was applied (Bensky 2008). Since the measurement contained a bias error, Root Mean Square (RMS) errors of 3D positioning and attitude and mean errors at the center of the positioning space were analyzed for accurate comparison.

The results of Experiments 1 and 2 were compared to analyze the positioning performance according to the number of APs. Figs. 7a-d show the 3D positioning and attitude errors in TOA-FLAOA and differenced FLAOA-TOA integrated techniques in Experiment 1, and Figs. 8a-d show the results of Experiment 2. The TOA-FLAOA integrated technique had about 0.15 m positioning error and 1.5° (in the

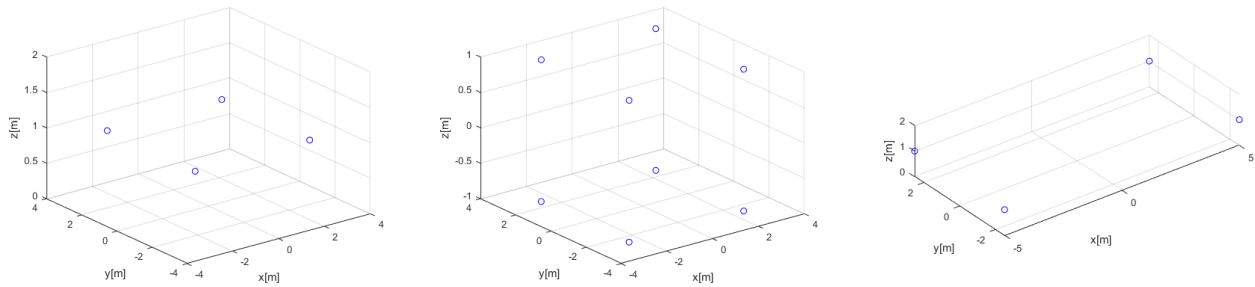


Fig. 6. Placement of APs in each experiment (left: experiment 1, middle : experiment 2, right : experiment 3).

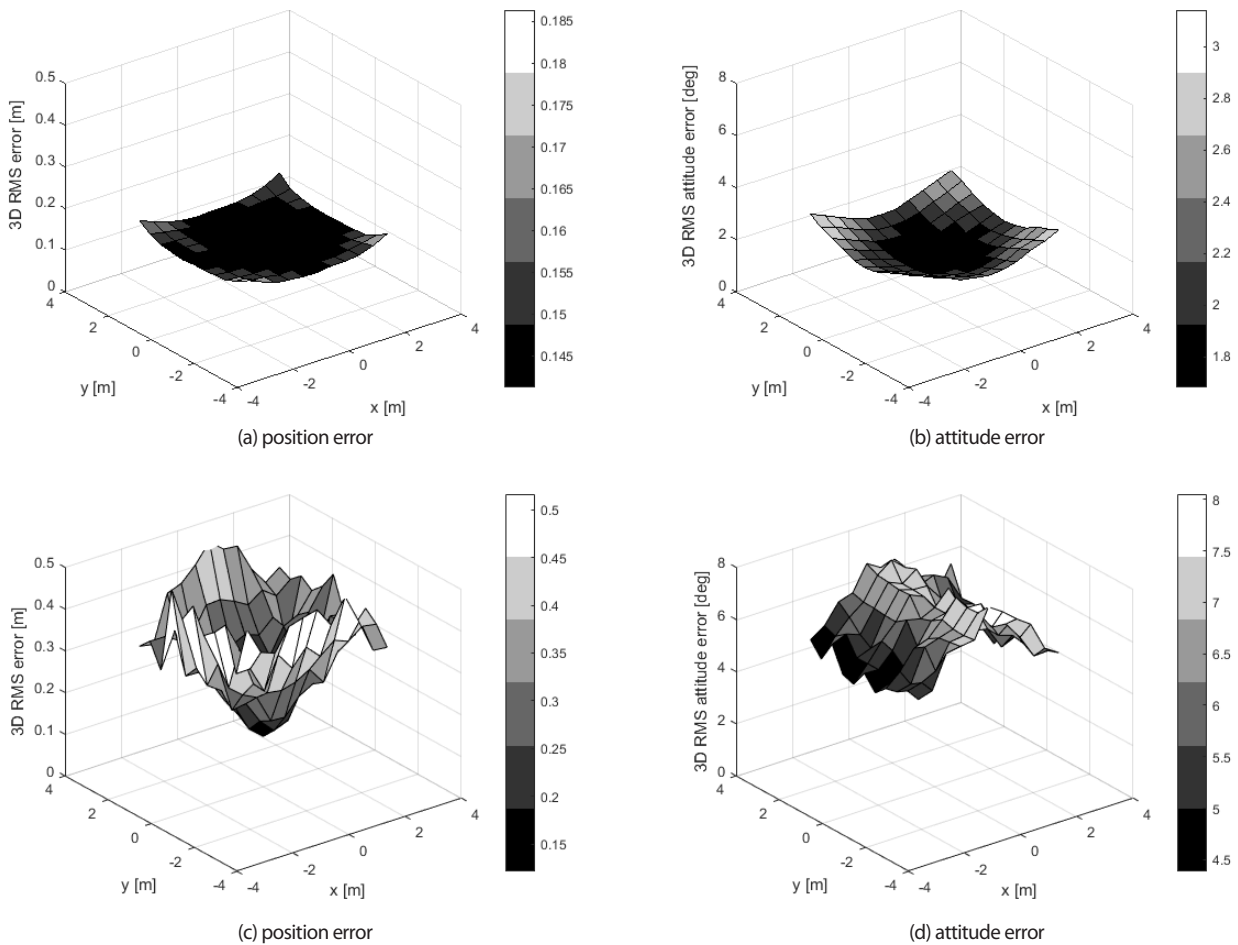
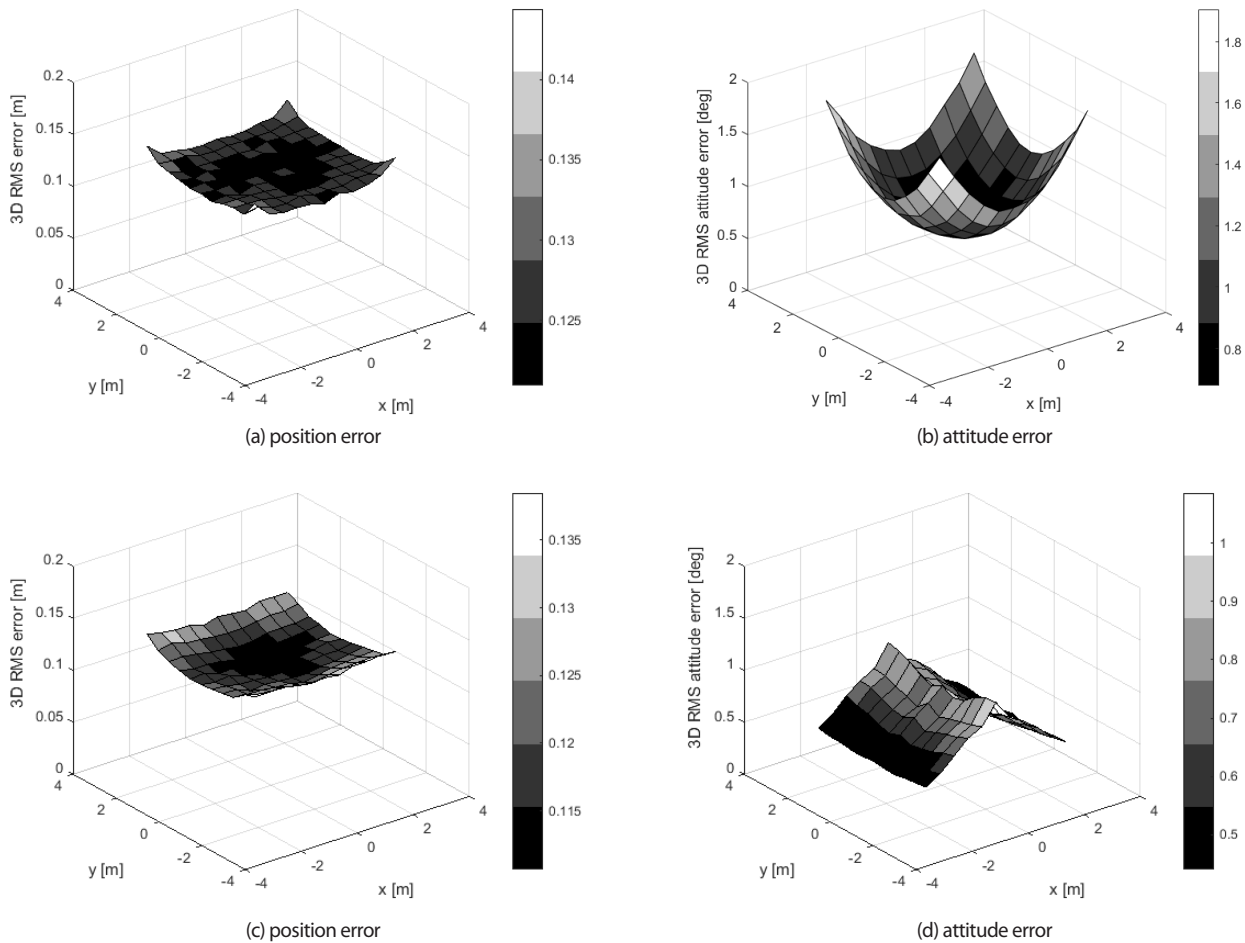


Fig. 7. The positioning error in FLAOA/TOA integrated system with 4 APs. (a) is result of positioning error using TOA-FLAOA integrated technique in experiment 1, (b) is result of attitude error using TOA-FLAOA integrated technique in experiment 1, (c) is result of positioning error using differenced FLAOA-TOA integrated technique in experiment 1, (d) is result of attitude error using differenced FLAOA-TOA integrated technique in experiment 1.

center part) to 3.0° (in the outer part) attitude error when the number of APs was four, and about 0.15 m positioning error and 0.5° (in the center part) to 2.0° (in the outer part) attitude error when the number of APs was eight. Thus, relatively uniform performances of positioning and attitude errors were revealed regardless of the tag position inside the positioning space, and no significant effect of the change in the number of

APs was exhibited. In contrast, the differenced FLAOA-TOA integrated technique had about 0.1 m (in the center part) to 0.5 m (in the outer part) positioning error and 5.0° (in the outer part) to 7.0° (in the center part) attitude error when the number of APs was four, and about 0.13 m positioning error and 0.5° (in the outer part) to 1.0° (in the center part) attitude error when the number of APs was eight. This technique



**Fig. 8.** The positioning error in FLAOA/TOA integrated system with 8 APs. (a) is result of positioning error using TOA-FLAOA integrated technique in experiment 2, (b) is result of attitude error using TOA-FLAOA integrated technique in experiment 2, (c) is result of positioning error using differenced FLAOA-TOA integrated technique in experiment 2, (d) is result of attitude error using differenced FLAOA-TOA integrated technique in experiment 2.

showed equivalent or superior positioning performance than TOA-FLAOA integrated technique when the number of APs was sufficient. In contrast, when the number of APs was insufficient, the positioning errors became about three times larger and attitude errors became about seven to ten times larger than those when the number of APs was sufficient, indicating rapid performance degradation. Thus, changes in positioning error were significantly large according to the position of the tag.

Next, the results of Experiments 1 and 3 were compared to analyze the positioning performance according to the arrangement of the positioning network. Figs. 9a-d show the experiment results of the two techniques in Experiment 3. Since the positioning space was a rectangular shape in Experiment 3, the area where the DOP was bad in the positioning space was large. Thus, positioning errors in both of the techniques were larger than those of Experiment 1 but the overall pattern was similar to that of Experiment

1. In TOA-FLAOA integrated technique, positioning error was relatively uniform inside the positioning space. The positioning and attitude errors of Experiment 3 were increased by about 1.1 times and 1.2 times respectively, compared to that of Experiment 1. In contrast, in the differenced FLAOA-TOA integrated technique, positioning and attitude errors of Experiment 3 were increased by about 1.5 to 3 times and 1.6 times respectively, compared to that of Experiment 1 as a measurement place became farther from the center of the positioning space.

The mean values of positioning and attitude errors were compared to analyze the errors quantitatively. Tables 2 and 3 present the mean values of positioning and attitude errors at positions (0, 0, 0) and (2.5, 2.5, 0) of the tag in Experiments 1 to 3. Both of the techniques showed a similar performance in the center of the positioning space whereas positioning errors were diverged as a measurement place became farther away from the center of the space in the case of differenced

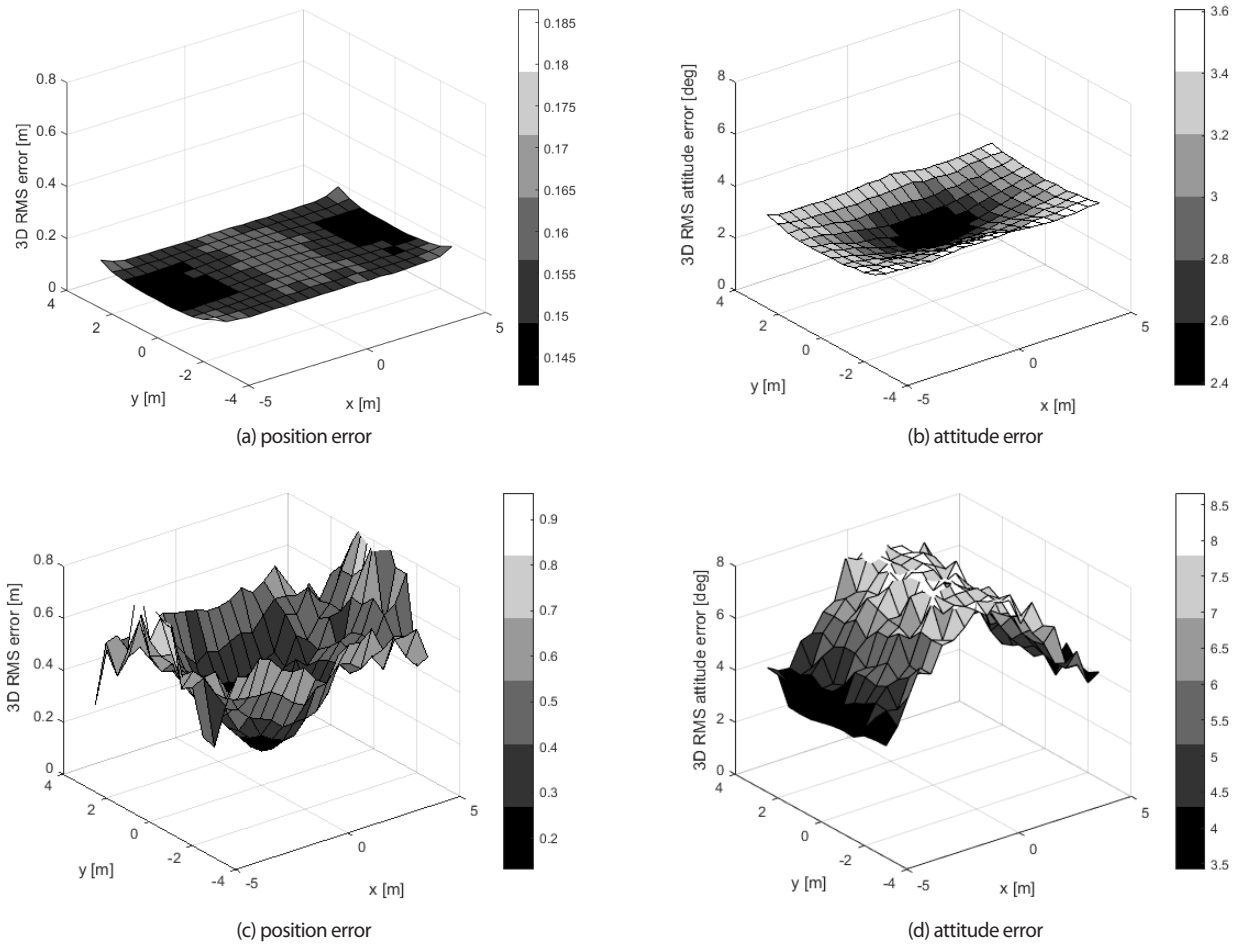


**Fig. 9.** The positioning error in FLAOA/TOA integrated system for bad DOP. (a) is result of positioning error using TOA-FLAOA integrated technique in experiment 3, (b) is result of attitude error using TOA-FLAOA integrated technique in experiment 3, (c) is result of positioning error using differenced FLAOA-TOA integrated technique in experiment 3, (d) is result of attitude error using differenced FLAOA-TOA integrated technique in experiment 3.

**Table 2.** The average of the position and attitude errors at the tag position (0, 0, 0).

		TOA-FLAOA integrated technique		differenced FLAOA-TOA integrated technique	
		Position error [m]	Attitude error [deg]	Position error [m]	Attitude error [deg]
<i>Experiment 1</i>	<i>x</i>	-0.001	0.0488	0.0002	0
	<i>y</i>	0.0037	0.1339	-0.0027	0
	<i>z</i>	0.0017	-0.0555	0.0006	-0.1989
<i>Experiment 2</i>	<i>x</i>	0.001	0.0071	0.0011	0
	<i>y</i>	0.0036	0.0055	-0.0004	0
	<i>z</i>	0.0024	0.0233	0.0042	0.0313
<i>Experiment 3</i>	<i>x</i>	0.0016	0.129	0.0043	0
	<i>y</i>	0.0005	0.1624	0.0022	0
	<i>z</i>	-0.0019	0.0357	0.0017	-0.1335

FLAOA-TOA integrated technique.

Finally, a size of the positioning space in Experiments 1 to 3 was expanded by one to ten times to analyze the positioning performance of the two techniques according to a size of positioning space, and positioning and attitude errors at tag position (0,0,0) were compared. Figs. 10a-d show the 3D positioning and attitude errors of the two techniques according to the expansion of the workspace size. The

attitude error in TOA-FLAOA integrated technique had a range of 0.5° to 2.5° due to the DOP or the number of APs, and the positioning error had no significant change around 0.15 m and no significant effect of the expansion of positioning space was revealed. In contrast, the positioning error in the case of differenced FLAOA-TOA integrated technique was affected by DOP or the number of APs significantly. In particular, the attitude error was increased by seven to ten times compared



**Table 3.** The average of the position and attitude errors at the tag position (2.5, 2.5, 0).

TOA-FLAOA integrated technique			differenced FLAOA-TOA integrated technique		
	Position error [m]	Attitude error [deg]	Position error [m]	Attitude error [deg]	
Experiment 1	x	0.0017	-0.0099	0	
	y	-0.0003	-0.0161	0	
	z	-0.0019	-0.0067	-0.0017	-0.1091
Experiment 2	x	-0.0029	-0.05	-0.004	0
	y	-0.0021	0.0724	-0.0037	0
	z	0.008	-0.0436	0.0018	0.0085
Experiment 3	x	0.0014	0.1528	-0.0371	0
	y	-0.0012	0.1286	-0.0502	0
	z	-0.0011	0.0125	-0.0053	-0.2121

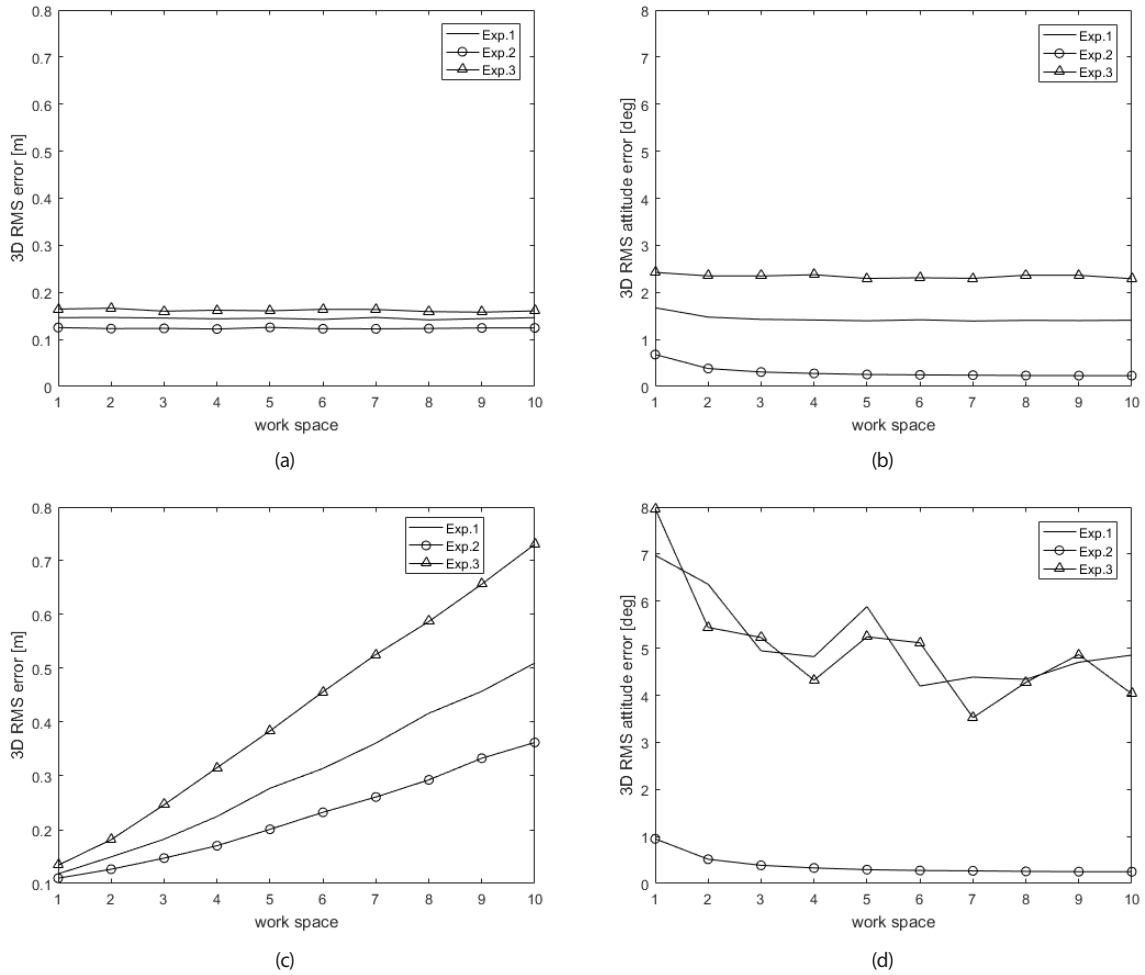


**Fig. 10.** The positioning error according to size of work space (tag position is (0,0,0)). (a) is positioning error result of experiment 1~3 using TOA-FLAOA integrated technique, (b) is attitude error result of experiment 1~3 using TOA-FLAOA integrated technique, (c) is positioning error result of experiment 1~3 using differenced FLAOA-TOA integrated technique, (d) is attitude error result of experiment 1~3 using differenced FLAOA-TOA integrated technique.

to good positioning environment. In addition, the figures verified that the attitude error was not affected significantly when the size of positioning space became larger but the positioning error was increased rapidly by 3.5 to 5.5 times when the size of positioning space became ten times larger.

In the differenced FLAOA-TOA integrated technique, positioning errors were not uniform when the number of APs

was insufficient or DOP was bad, and positioning errors were rapidly increased as the positioning space became larger. The reason for those phenomena is as follows: since the differenced FLAOA-TOA integrated technique differentiates FLAOA measurement, increase rates of positioning and attitude errors are high when the number of APs is small or DOP is poor. In addition, since the position is calculated

after estimating the attitude first using the differential measurement, the attitude estimation error will have an effect on amplifying the positioning error significantly as DOP is poor or a distance between tag and AP become farther. Thus, a positioning error increases rapidly as a positioning space size becomes larger. In contrast, TOA-FLAOA integrated technique showed consistent and excellent positioning performance in all workspaces regardless of the number of APs, DOP, and the size of positioning space.

## 5. CONCLUSIONS

This paper proposed a radio navigation system to determine 3D position and attitude of moving vehicles by integrating FLAOA and TOA measurements. The TOA-FLAOA integrated technique that calculated attitude from FLAOA measurements after calculating a position from TOA measurements, and the differenced FLAOA-TOA integrated technique that calculated a position after calculating attitude from the differenced FLAOA measurement were proposed. The simulation results showed that the differenced FLAOA-TOA integrated technique was sensitive to the number of APs or DOP and positioning error was rapidly increased according to the size of positioning space whereas TOA-FLAOA integrated technique revealed consistent and excellent positioning and attitude determination performances in all positioning spaces regardless of the number of APs, DOP, and positioning space size. Thus, when TOA-FLAOA integrated technique proposed in IR-UWB radio positioning system is applied, it can calculate high precision positioning and attitude of indoor moving vehicles at the same time and it can be applied to various indoor navigation applications.

## ACKNOWLEDGMENTS

This work was supported by research fund of Chungnam National University.

## REFERENCES

- Bensky, A. 2008, *Wireless Positioning Technologies and Applications* (Boston, MA: Artech House)
- Hu, B. 2013, *Wi-Fi Based Indoor Positioning System Using Smartphones*, Master's Thesis, Royal Melbourne Institute of Technology (RMIT) University
- Kim, D. H., Song, S. H., Roh, G. H., & Sung, T. K. 2007, A Forward Link AOA Positioning method for mobile

Robots, *Journal of Control, Automation and Systems Engineering*, 13, 603-608. <http://www.dbpia.co.kr/Journal/ArticleDetail/NODE01975775>

- Lim, J. M. 2017, *Study on FLAOA-based Position and Attitude Determination with Sensor-fusion*, Ph.D Thesis, Chungnam National University
- Mardiana, R. & Kawasaki, Z. 2000, Broadband radio interferometer utilizing a sequential triggering technique for locating fast-moving electromagnetic sources emitted from lightning, *IEEE Transactions on Instrumentation and Measurement*, 49, 376-381. <https://doi.org/10.1109/19.843081>
- Sahinoglu, Z., Gezici, S., & Güvenc, I. 2008, *Ultra-wideband Positioning Systems: Theoretical Limits, Ranging Algorithms, and Protocols* (Cambridge: Cambridge University Press)
- Song, S. H., Im, H. J., Park, J. W., & Sung, T. K. 2009, A New Angle-Based Location Method Using a Forward-Link Signal, *EURASIP Journal on Advances in Signal Processing*, Vol. 2009, 6 pages. <https://doi.org/10.1155/2009/407893>
- Swedberg, C. 2016, Ubisense Introduces AngleID to Provide Low-Cost, Real-Time Zone Location, *RFID Journal*, 2016 RFID Journal Articles. <http://www.rfidjournal.com/articles/view?14477>
- Titterton, D. & Weston, J. L. 2004, *A Strapdown Inertial Navigation Technology*, 2nd Ed. (Reston: AIAA)
- Van Graas, F. & Braasch, M. 1991, GPS GPS Interferometric Attitude and Heading Determination: Initial Flight Test Results, *Journal of the Institute of Navigation*, 38, 297-316. <https://doi.org/10.1002/j.2161-4296.1991.tb01864.x>
- Viot, M. 2014, IOT 2.0: When the IOT and micro location converge, 2014 IOT Conference, July 13-18, 2014, San Diego, CA. [http://www.ieee802.org/802\\_tutorials/2014-07/bof\\_viot\\_14\\_0716.pdf](http://www.ieee802.org/802_tutorials/2014-07/bof_viot_14_0716.pdf)
- Zhu, L., Yang, A., Wu, D. & Liu L. 2014, Survey of Indoor Positioning Technologies and Systems, *LSMS/ICSEE 2014, Communications in Computer and Information Science*, 461, 400-409. [https://doi.org/10.1007/978-3-662-45283-7\\_41](https://doi.org/10.1007/978-3-662-45283-7_41)



**Jong-Hwa Jeon** is a master course in the Department of Electronics, Radio Sciences and Information Communications Engineering at Chungnam National University. He received his B.S degree from Chungnam National University in 2016. His research interests are RTK, FLAOA and UWB.



**Jeong-Min Lim** received M.S., and Ph.D. degree in Electronics, Radio Sciences & Engineering and Information Communications Engineering from Chungnam National University, Korea, in 2013, and 2017, respectively. He served at Wifive research institute from 2014 to 2017. Where he is currently a researcher of MTG technical research center. His research interest is RADAR.



**Sang-Hoon Yoo** received M.S degree in Information and Communication Engineering from Chungnam National University in 2015. He is currently a researcher in WiFive Co. Ltd. His research interests are GPS/GNSS, Indoor Positioning and Map-Matching.



**Tae-Kyung Sung** received B.S., M.S., and Ph.D. degree in control and instrumentation engineering from Seoul National University. After working at the Institute for Advanced Engineering, and Samsung Electronics Co., he joined the Chungnam National University, Daejeon, Korea, where he is currently a Professor of the Division of Electrical and Computer Engineering. He participated in several research projects in the area of positioning and navigation systems. His research interests are GPS/GNSS, Geo-location, UWB WPAN positioning, and location signal processing.